Resonance Topology and Related Aspects of Fluoranthenoid / Fluorenoid and Indacenoid Hydrocarbon Radicals

Gordon G. Cash and Jerry Ray Dias[a]

Risk Assessment Division (7403M), Office of Pollution Prevention & Toxics, U. S. Environmental Protection Agency, 1200 Pennsylvania Avenue, N. W., Washington, D. C. 20460, U. S. A.
[a] Department of Chemistry, University of Missouri, Kansas City, MO 64110-2499, U. S. A.

Reprint requests to G. C.: E-mail: cash.gordon@epa.gov

Z. Naturforsch. **57 a,** 650–660 (2002); received February 5, 2002

Data on the number of resonance structures of free radical polycyclic conjugated hydrocarbons are tabulated and studied. The first examples of fluoranthenoid / fluorenoid and indacenoid polyradical systems are presented. Some comparative generalizations between benzenoid free radicals and fluoranthenoid / fluorenoid and indacenoid polyradical systems are formulated. For example, there is a tendency of these latter even-carbon nonalternant hydrocarbons to have fewer radical isomers compared to the former alternant hydracarbons. Examples where Fowler's leapfrog algorithm identifies the more stable fluorenoid anion and indacenoid dianion isomer are presented.

Key words: Resonance Topology; Hydrocarbon Radicals; Structure Count.

Introduction

Fluoranthenoids / fluorenoids are even/odd carbon polycyclic conjugated hydrocarbon molecules composed of one pentagonal ring ($r_5 = 1$) among otherwise hexagonal rings, and indacenoids (dicyclopenta-fused polycyclic aromatic hydrocarbons) are polycyclic hydrocarbon molecules composed of two pentagonal rings ($r_5 = 2$) among otherwise hexagonal rings. In addition to benzenoid hydrocarbons and fullerenes, these are among the molecules prevalently formed in fuel pyrolysis and combustion processes.

Since the appearance of our work on fluoranthenoid / fluorenoid [1] and indacenoid [2] constant-isomer series, numerous other results [3] dealing with this phenomenon have been published. Moreover, there exists an extensive research literature [4] on the determination of the number of Kekulé resonance structures of benzenoid and closely related hydrocarbons, whereas relatively little work on the topology and determination of the number of resonance structures of nonalternant hydrocarbons has been done. This void gives us the opportunity to systematically review our prior work while studying how structural changes in the members of these constant-isomer series affects their number of resonance structures. Fowler's leapfrog algorithm has been shown to identify the most stable fullerene [5] and benzenoid isomers [6], and its application to fluorenoids / fluoranthenoids and indacenoids was studied here to see if it can be used as a tool to identify the most stable members of these classes of molecules. In addition, regularities in changes in structure count (SC) with successive circumscribing within indacenoid and fluorenoid / fluoranthenoid constant-isomer series are investigated and described.

Terminology

Herein interlocking hexagons (polyhex graph) will be used to represent fused benzenoid molecules. A polypent / polyhex molecular graph consists of interlocking pentagons and hexagons where the degree-2 vertices correspond to methine >C-H units, and degree-3 vertices correspond to =C< carbon units. Thus, a molecular graph is the C-C s-bond representation of a conjugated polyene molecule where the number of degree-2 vertices, degree-3 vertices, edges, and rings are given by $N_H = s$, $N_c = n$, q, and r, respectively. The number of Kekulé resonance structures is designated by K, and the number of free-radical resonance structures is designated by SC.

Results and Discussion

Circumscribing Algorithm and Constant-Isomer Series

The excised internal structure / circumscribing principle is an extremely important concept which leads to constant-isomer series [1, 2, 7]. The circumscribing of ethene (C_2H_4) with a perimeter of 14 carbon atoms and supplementing with 6 hydrogen atoms in such a way as to generate only hexagonal rings with each atom fulfilling proper valence leads to pyrene ($C_{16}H_{10}$). Conversely, excising out the connected internal carbon vertices of pyrene with simultaneous transfer of 4 hydrogen atoms leads to ethene. Circumscribing and excision are reverse operations. Since there is only one C_2H_4 isomer (ethene), there can only be one benzenoid isomer of the formula of $C_{16}H_{10}$, namely pyrene. Circumscribing pyrene with a 26 carbon atom perimeter and supplementing with 6 more hydrogens gives the only $C_{42}H_{16}$ benzenoid possible, called circum(26)pyrene. Repeating this process indefinitely gives successive larger benzenoid members belonging to the D_{2h} (idealized geometry) one-isomer polycircumpyrene series. Similarly, circumscribing of benzene (C_6H_6) gives coronene ($C_{24}H_{12}$), and repeating this process successively leads to the D_{6h} coronene one-isomer benzenoid series. Successive circumscribing fluorenoids / fluoranthenoids [1] and indacenoids [2] with perimeters of hexagonal rings has also been shown to give constant isomer series. Members of constant-isomer series are the most compact polycyclic molecules of the given formula, have the fewest possible isomers, and have formulas on the extreme left-hand staircase boundary of the relevant formula periodic table.

In general, constant-isomer series are generated by the successive circumscribing with hexagonal rings and are infinite sets of polycyclic conjugated hydrocarbons with increasing numbers of carbon and hydrogen atoms which have equal numbers of isomers at each stage of the increasing formula. For each circumscribing step, the initial N_c and N_H values are increased to N_c' and N_H per the equations

$$N_c' = N_c + 2N_H + 6 - r_5$$

and

$$N_H' = N_H + 6 - r_5,$$

where the number of pentagonal rings (r_5) remains constant. A necessary and sufficient condition to prevent the circumscribing of a polycyclic system is the presence of adjacent bay regions. We denote the circumscription of a polypent / polyhex (polyene) system by P $\rightarrow$ circum-P = P′. It has been previously shown that $r = (^1/_2)(N_c - N_H) + 1$, where $N_c = N_{pc} + N_{Ic} + N_H$, and where N_{pc}, N_{Ic} and q_p are the number of perimeter and internal degree-3 vertices and perimeter edges, respectively. For P $\rightarrow$ P′, $N_c \rightarrow N_{Ic}'$ and $N_H \rightarrow N_{pc}'$. Thus, for circum-P, $N_{pc}' = N_H' - 6 + r_5 = N_H$ giving $N_H' = N_H + 6 - r_5$ and, similarly, $q_p' = N_{pc}' + N_H'$ and $N_c' = q_p' + N_c$, giving $N_c' = N_c + N_{pc}' + N_H' = N_c + 2N_H + 6 - r_5$. These recursive equations are useful for monitoring the progress of successive circumscribing. As an specific example, consider cyclopentadienyl in Figure 1. Detaching all five hydrogens from cyclopentadienyl, attaching a cycle of fifteen carbons in such a way as to only form a perimeter of hexagonal rings, and reattaching the five hydrogens removed plus five additional hydrogens generates corannulene ($C_{20}H_{10}$); cyclopentadienyl and corannulene are the first two generation members of the most symmetrical fluoranthenoid / fluorenoid one-isomer series [1].

Also shown in Fig. 1 is the circumscribing process for indenyl and acenaphthylene which form the first two members of the remaining one-isomer series. It should be noted that repetitively circumscribing polycyclic hydrocarbons containing only one pentagonal ring gives an alternating fluorenoid / fluoranthenoid (odd / even number of carbons) constant-isomer series. Fluorenoid (odd carbon) hydrocarbons are always radical systems. Figure 2 shows the first two generation members for the three indacenoid one-isomer series. The indacenoid one-isomer series starting with pentalene is made up of even carbon members and the other two one-isomer series have odd carbon members and are monoradicals.

The smallest most compact polyradical benzenoid hydrocarbons were shown to be shaped like *equilateral triangles* (D_{3h}) with the general formula of C_nH_s ($n = t^2 + 6t + 6$, $s = 3t + 6$, $t = 1, 2, 3, \ldots$ = radical degree) which starts with phenalenyl monoradical ($t = 1$) [8]. The related fluorenoid / fluoranthenoid polyradicals are generated from these triangular systems by contracting one of their apex hexagonal rings to a pentagonal ones, resulting in the fluorenoids / fluoranthenoids shown in Figure 3. For each hexagonal ring contracted to a pentagonal one, the radical degree is reduced by one. Thus by this transformation,

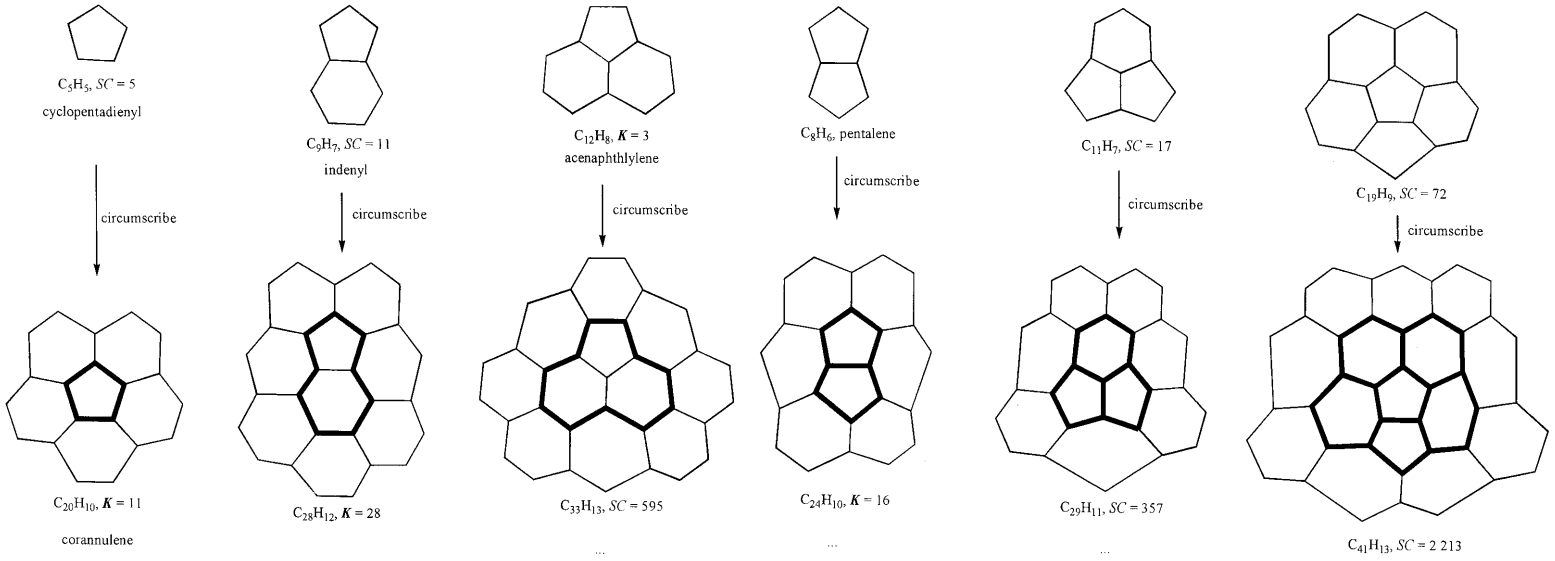

Fig. 1. First and second generation members of the fluorenoid / fluoranthenoid one-isomer series. The excised internal structures of the second generation members are shown in bold. The recursion formulas for circumscribing fluorenoids / fluoranthenoids are $N_c' = N_c + 2N_H - 5$ and $N_H' = N_H + 5$.

Fig. 2. The circumscribing / excised internal structure concept in the successive generation of the members belonging to the three indacenoid one-isomer series; e. g., circumscribing pentalene gives circum[16]pentalene ($C_{24}H_{10}$), and pentalene is the excised internal structure of circum[16]pentalene. The recursion formulas for circumscribing indacenoids are $N_c' = N_c + 2N_H - 4$ and $N_H' = N_H + 4$.

Fig. 3. Smallest most condensed fluorenoid / fluoranthenoid polyradical series. ⟶

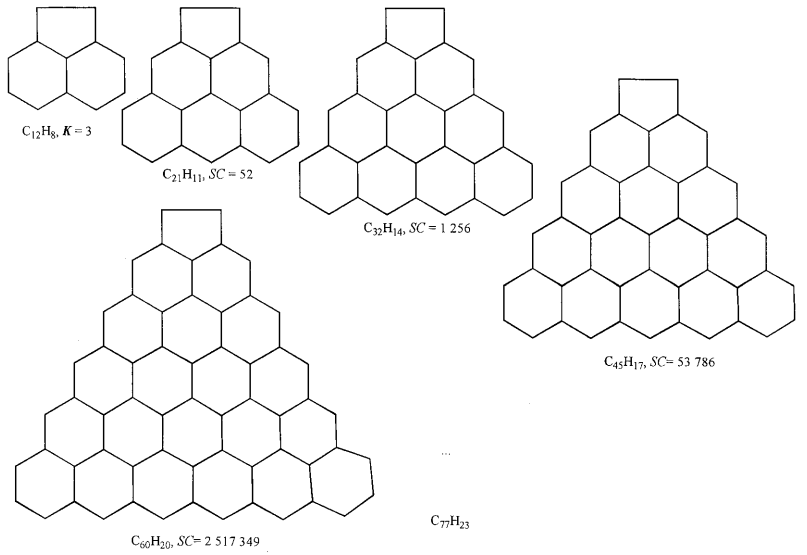

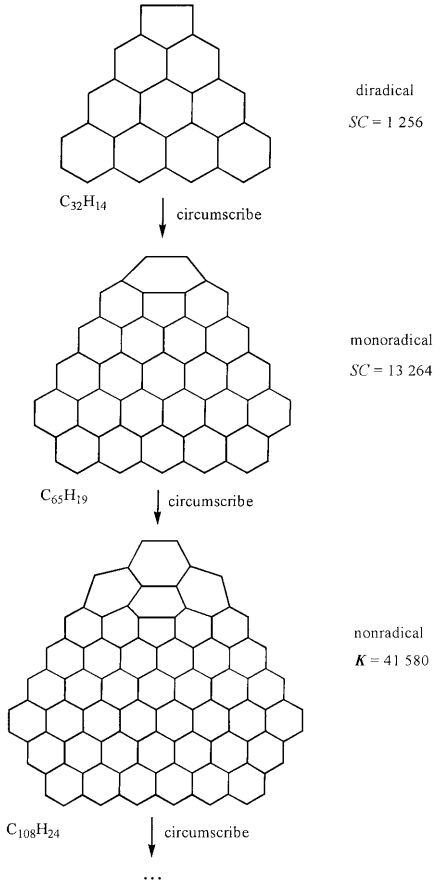

Fig. 4. Successive circumscribing the smallest diradical fluorenoid / fluoranthenoid.

phenalenyl monoradical ($C_{13}H_9$, $t = 1$) becomes the nonradical, acenaphthylene ($C_{12}H_8$), and triangulene diradical ($C_{22}H_{12}$, $t = 2$) becomes the $C_{21}H_{11}$ fluorenoid monoradical (second structure) shown in Figure 3. The $C_{32}H_{14}$ fluoranthenoid in Fig. 3 is an isomer of ovalene and is the smallest diradical fluoranthenoid hydrocarbon possible. Figure 4 shows that two successive circumscribings of this $C_{32}H_{14}$ fluoranthenoid results in a nonradical (Kekulean) fluoranthenoid hydrocarbon ($C_{108}H_{24}$). This result is in marked contrast with the triangular benzenoid polyradicals in which radical degree is unchanged upon successive circumscribing [8].

The above shows that successive circumscribing of fluorenoids / fluoranthenoids results in successive alternation in their monoradical and nonradical character, and that a higher radical degree is obliterated by this process.

Contracting another corner hexagon ring to a pentagon ring in the molecular graphs of the fluorenoid / fluoranthenoid series in Fig. 3 results in the indacenoid series given in Figure 5. The $C_{44}H_{16}$ indacenoid structure is a diradical, and the $C_{59}H_{19}$ indacenoid structure is a triradical. It was previously shown that the smallest indacenoid diradical (first molecular graph in Fig. 6) is a D_{2h} isomer of a semibuckminsterfullerene ($C_{30}H_{12}$) which has a 2,5-dimethylenylpentalene diradical (shown in bold in Fig. 6) as its excised internal structure [2]. Triangulene ($C_{22}H_{12}$) is the smallest benzenoid diradical which has the smallest alternant diradical (trimethylenemethane) as an excised internal structure. The $C_{30}H_{12}$ molecular graph in Figure 6 is the smallest indacenoid diradical which has the smallest nonalternant diradical with two pentagonal rings as an excised internal structure. This latter diradical (2,5-dimethylenylpentalene) can be embedded by trimethylenemethane and is subspectral in its eigenvalues. Repetitive circumscription of any of the diradicals in Fig. 6 results in successor diradical fluoranthenoids.

Regularities in SC with Successive Circumscribing

For closed-shell structures ($\boldsymbol{K} > 0$) that can be represented as planar graphs, $\boldsymbol{K}$ is easily determined via the signed adjacency matrix [9] for structures of arbitrary size. For radicals ($\boldsymbol{K} = 0$), other approaches must be used to obtain structure counts.

Using a differential-operator-based algorithm conceived by Rosenfeld and Gutman [10] and developed by Salvador et al. [11], combined with an equation for fragmentation published by Babić et al. [12], it is possible to calculate matching (acyclic) polynomials for structures of moderate size, say ~120 non-hydrogen atoms. This method is applicable to structures of any radical multiplicity, since the last term in that polynomial, $a_i x^j$, contains the structure count ($SC = a_i$) and the radical multiplicity (j).

For the present study, we needed *SC*s for larger structures (~300 non-hydrogen atoms), some of which were monoradicals. To this end, we developed an algorithm that takes advantage of an obvious relationship: The structure count for a monoradical is just the sum of the Kekulé counts for structures with the radical center isolated on each atom available to it. Thus, if the unpaired electron can reside on any of n possible sites, the *SC* for the radical is the sum of n $\boldsymbol{K}$

Fig. 5. Smallest most condensed indacenoid polyradical series.

Fig. 6. Indacenoid diradical series and their number of resonance structures (*SC*).

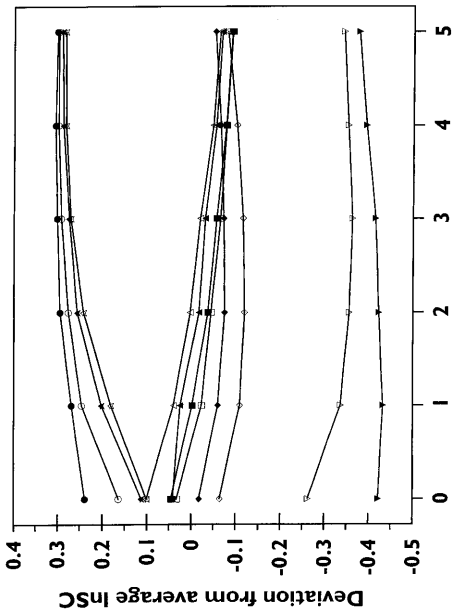

Fig. 7. Plot of number of circumscribings vs. deviation from average ln *SC* for the two six-isomer indacenoid series. Hollow symbols are used for members of the first series, and the corresponding filled symbols are used for corresponding members of the second series. The relationship between corresponding members is immediately obvious.

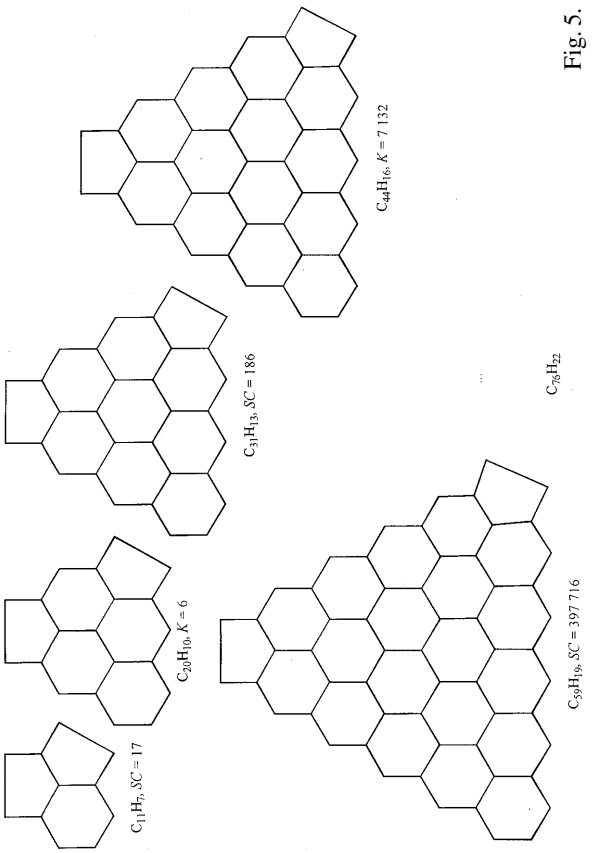

Fig. 5.

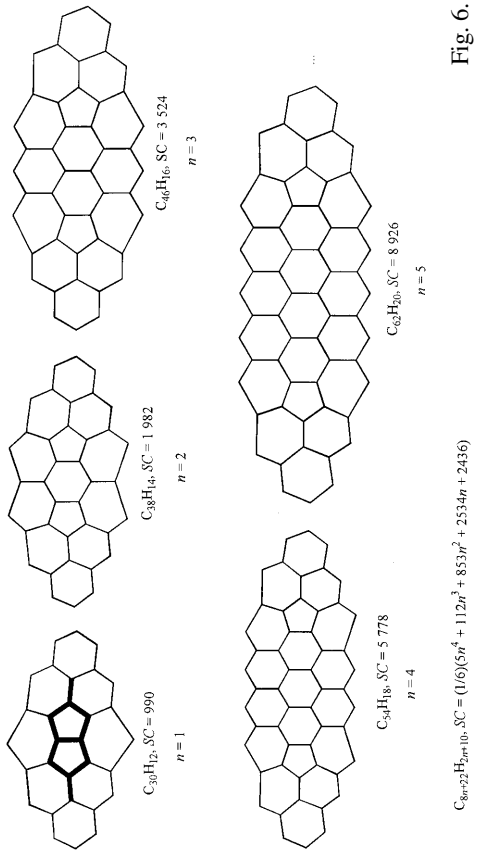

Fig. 6.

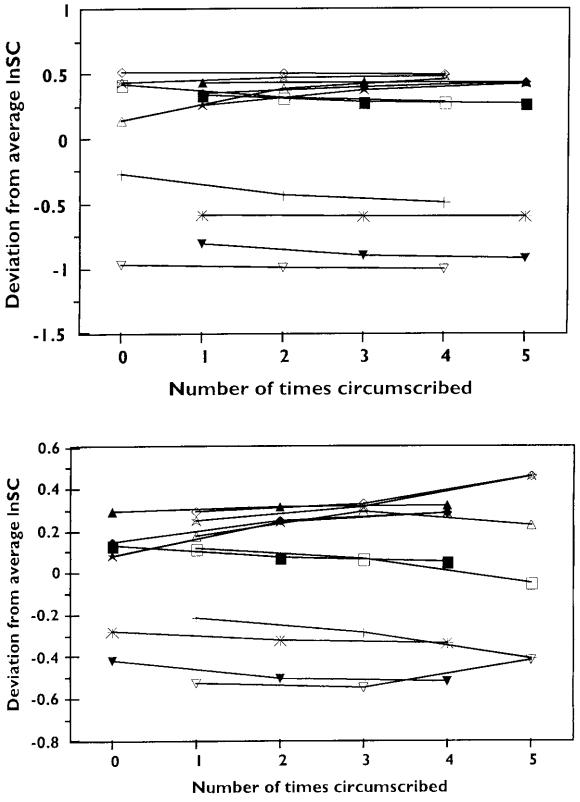

Fig. 8. Plot of number of circumscribings vs. deviation from average ln *SC* for six pairs from the two seven-isomer fluorenoid / fluoranthenoid series. For one isomer, + and ∗ serve, respectively, as the hollow and filled symbols. The plots are separated into even-carbon species (upper) and odd-carbon species (lower). Plotted together, the two sets of lines would have a zig-zag, rather than parallel, relationship because the radical multiplicities do not match; see text.

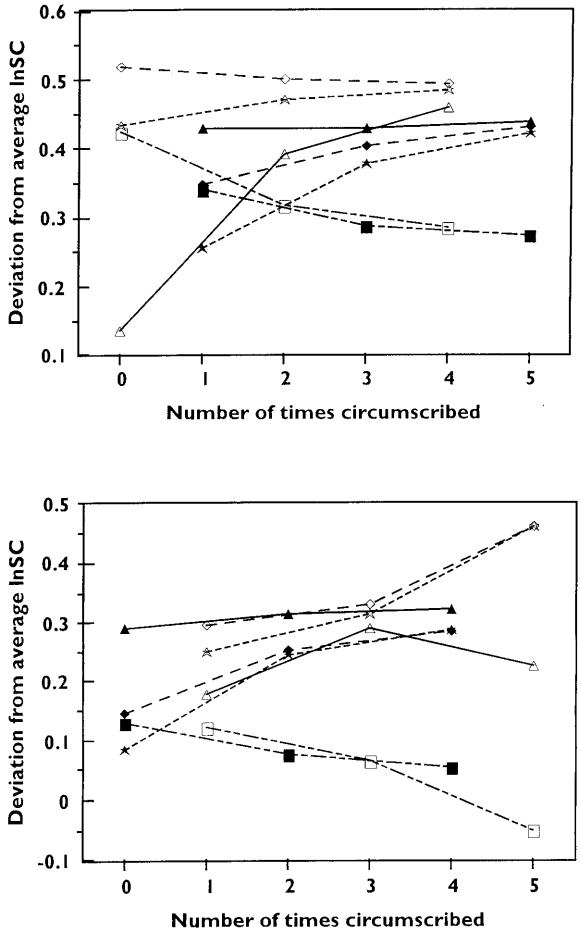

Fig. 9. The top portions of Fig. 8 are expanded, and different line styles are used, to facilitate comparisons. Four of the seven members from each series are shown.

values, each of which is calculable from its signed adjacency matrix. The signed adjacency matrix for the case with the radical on the i^{th} vertex is just the signed adjacency matrix for the entire structure with the i^{th} column and row deleted. By a judicious choice of vertex numbering it is possible to automate the process of generating these matrices and obtain *SC*s for quite large monoradicals. Although theoretically applicable to higher radical multiplicities, this algorithm is practical only for monoradicals. Nevertheless, it was adequate for the present study of successive circumscribing. Since each base structure must be handled slightly differently, all results were checked against the matching polynomial for the largest structures for which the polynomial could be calculated.

*SC*s were obtained for the two six-isomer indacenoid series [2] and the two seven-isomer fluorenoid / fluoranthenoid series [1], with each base structure circumscribed with hexagons 0-5 times. Structure diagrams may be found as Fig. 5 in [2d] and Fig. 6 and 7 in [1b], respectively. Table 1 lists the individual *Sc*s. Within each two series (indacenoid, fluorenoid/fluoranthenoid), the isomers occur naturally in pairs, one in each series with regard to definitive structural features, e. g., adjacency / nonadjacency of the pentagons for the indacenoids, presence or absence of a bay region, symmetry, in the base structures.

When ln *SC* is plotted against the number of times circumscribed, little difference is apparent among the various structures. The pairing of structures is very

Table 1. SCs for the two 6-isomer indacenoid and the two 7-isomer F/F series, circumscribed $n-1$ times (n = 0 is the uncircumscribed structure). Designations refer to Fig. 5 of [7d] ($C_{17}H_9$ and $C_{27}H_{11}$ series), Fig. 6 of [1b] ($C_{26}H_{12}$ series), and Fig. 7 of [1b] ($C_{31}H_{13}$ series).

n	$C_{17}H_9$ series SCs	$C_{27}H_{11}$ series SCs	n	$C_{17}H_9$ series SCs	$C_{27}H_{11}$ series SCs
First structure, top left:			Second structure, top right:		
1	46	229	1	32	144
2	1 490	11 577	2	1 022	7 330
3	114 348	1 418 745	3	79 832	945 376
4	23 172 516	473 268 784	4	16 431 120	322 451 856
5	12 453 925 344	423 486 993 990	5	9 185 462 352	301 966 110 672
6	18 709 651 404 912	1 061 452 531 083 092	6	14 159 388 640 528	779 996 508 656 808
Third structure, middle left:			Fourth structure, middle right:		
1	43	230	1	39	216
2	1 400	11 276	2	1 284	10 640
3	109 047	1 389 774	3	101 068	1 337 912
4	22 116 772	461 251 967	4	21 038 012	453 869 812
5	12 076 258 672	413 912 087 480	5	11 808 689 501	419 257 067 014
6	18 196 643 335 322	1 037 788 796 685 344	6	18 387 707 121 160	1 077 906 073 127 952
Fith structure, bottom left:			Sixth structure, bottom right:		
1	49	279	1	46	246
2	1 832	14 781	2	1 716	13 824
3	150 196	1 927 120	3	145 232	1 863 513
4	31 649 360	659 460 364	4	30 971 976	642 026 353
5	17 628 172 636	607 524 591 206	5	17 330 574 568	597 184 607 738
6	26 881 405 644 614	1 536 038 999 762 118	6	26 476 209 934 636	1 519 284 882 432 032

n	$C_{26}H_{12}$ series SCs	$C_{31}H_{13}$ series SCs	n	$C_{26}H_{12}$ series SCs	$C_{31}H_{13}$ series SCs
First structure, top left:					
1	15	491			
2	15 844	2 331			
3	140 820	16 626 489			
4	3 965 829 750	376 578 917			
5	198 203 963 503	72 954 944 856 635			
6	135 855 363 013 397 492	11 428 359 635 884 975			
Second structure, top center:			Third structure, top right:		
1	5	241	1	20	418
2	7 842	676	2	14 969	2 135
3	35 124	7 352 390	3	130 704	13 126 886
4	1 704 637 438	100 564 513	4	3 166 125 251	327 314 856
5	166 815 038 390	55 796 053 531 944	5	45 879 700 139	31 331 989 155 109
6	71 023 333 663 940 102	2 935 797 206 803 524	6	103 014 742 805 332 115	9 710 664 623 442 055
Fourth structure, middle left:			Fith structure, middle right:		
1	22	389	1	10	424
2	17 815	1 701	2	11 984	2 152
3	156 852	11 559 784	3	74 382	15 636 894
4	4 125 725 172	243 972 817	4	2 536 262 361	367 785 523
5	205 367 399 433	48 466 349 123 146	5	99 503 359 956	70 237 421 111 464
6	171 529 259 977 893 178	7 011 580 975 950 425	6	82 990 330 912 640 268	11 340 609 388 600 968
Sixth structure, bottom left:			Seventh structure, bottom right:		
1	20	399	1	10	277
2	17 026	1 961	2	10 700	848
3	152 268	15 520 443	3	61 692	8 765 974
4	4 063 275 801	358 233 539	4	2 216 042 065	134 856 869
5	203 317 892 505	70 436 885 307 435	5	76 888 249 893	37 785 181 475 343
6	171 869 006 635 853 550	11 244 457 718 228 609	6	71 803 628 250 816 764	4 064 589 636 697 800

obvious, however, when the ordinate variable is the difference between each ln *SC* and the average value for its constant-isomer series. Thus, for example, the six values for one constant-isomer indacenoid series circumscribe three times are averaged, and the variation from that average for each of the six values is plotted above the abscissa point for three circumscribings. Figure 7 shows the result of this exercise for all 72 indacenoid structures. To facilitate the comparison, a different hollow symbol is used for each isomer in the first series, and the corresponding filled symbol is used for the corresponding isomer in the second series. It is immediately obvious that each line tracks its corresponding isomer line better than it tracks any other line in the graph. We consider this a conclusive demonstration that the perceived relationships between these two constant-isomer series are real and not merely coincidental similarities of molecular shape. Comparison of Fig. 7 with Table 1 reveals that the two pairs of lines at the top of the plot correspond to the two pairs of structures with bay regions (bottom left and right in [7d]). There is no obvious structural rationale, however, for the single pair of lines at the bottom of Figure 7. These structures have adjacent pentagons, but this is also true of other structures in the set.

The situation with the two seven-isomer fluorenoid / fluoranthenoid series is not so straightforward because in one series the even-circumscribed members are closed-shell, while the odd-circumscribed members are radicals. In the other series, the opposite is true. Because of this, values of deviation from the average ln*SC* tend to alternately increase and decrease in going from one circumscribing to the next, and each isomer is out of phase with its counterpart in the other series. Nevertheless, Fig. 8 shows a pattern of lines that cross and recross, tracking each other in a zig-zag rather than parallel fashion. The top part of Fig. 8 is rather busy, so it is expanded in Fig. 9, and different line styles are used as well as different symbols to facilitate comparison. Even then, the pairing is not quite as apparent as with the two indacenoid series. Curiously, there is also one pair from the seven-isomer series that does not fit the pattern. This pair was deliberately omitted from Figs. 8 and 9, but is presented in Figure 10. There does not seem to be any obvious reason for this result, since the two structures appear to be quite similar. Perhaps the result is evidence that structural pairing is not applicable to all members of all sets of constant-isomer series. Clearly, more structures need to be studied in order to resolve this issue.

Leapfrog Algorithm

The leapfrog transformation was developed by Fowler as a tool to identify the more stable fullerenes [5]. There are 1812 fullerene isomers of C_{60}, and the leapfrog of the dodecahedron fullerene (C_{20}) identifies the icosahedral buckminsterfullerene as the most stable isomer [13]. While buckminsterfullerene has 12 500 Kekulé resonance structures ($\boldsymbol{K}$ = 12 500), there are 20 other C_{60} isomers with more resonance structures [14]. The origin of the greater stability of buckminsterfullerene has been attributed to the fact that amongst the 1812 structural isomers, it is the only isomer that has a Fries Kekulé structure where all hexagons contain three double bonds and all pentagons none [14]. Since all the carbon sites of buckminsterfullerene are equivalent, addition of hydrogen radical to buckminsterfullerene gives $C_{60}H$ monoradical which has more than 11 times as many resonance structures (*SC* = 140 092). The known azafullerene [15] analog ($C_{59}N$) also has this number of non-zwitterionic resonance structures.

The leapfrogging of any benzenoid leads to a total resonant sextet benzenoid (TRS) which has a maximum number of Clar sextets (disjoint hexagon rings with three mutually permutable pπ bonds) [6]. Total resonant sextet benzenoid (TRS) systems (called fully benzenoid systems by Clar) have formulas divisible by six and are totally covered by Clar sextets. The leapfrog transformation is of fundamental importance here because it allows us to identify the essentially strain-free benzenoid isomers predicted to be among the more kinetically stable ones (largest HOMO values) and with highest Hückel pπ electronic energy without knowledge of the remaining isomers [6]. All known TRS benzenoids are colorless crystals that do not react with concentrated sulfuric acid and are the isomers with the largest Hückel E_π and HOMO values. From an experimental and HMO point of view, TRS benzenoids represent a distinctive subset of benzenoids in general. Our previous work demonstrated that there exists a one-to-one matching between strictly peri-condensed and total resonant sextet constant-isomer series. In going from the parent P to its leapfrog L, the following correspondences hold:

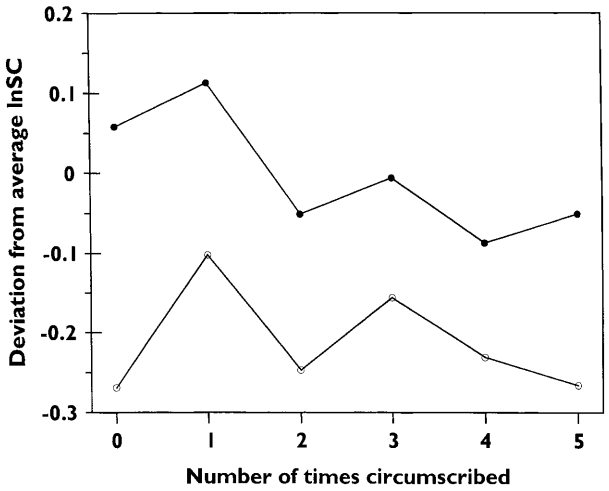

Fig. 10. One pair from the seven-isomer fluorenoid / fluoranthenoid series does not fit the pattern.

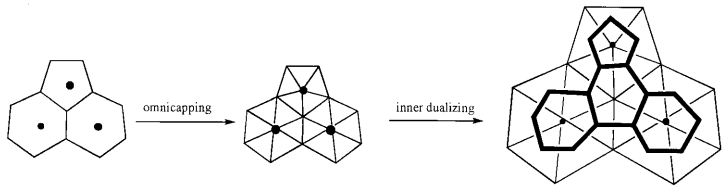

Fig. 12. Leapfrogging acenaphthylene gives dibenzo[*e,g*]indenyl. Omnicap by connecting ring centrix points to adjacent ring vertices. Then obtain the inner dual by placing points in all the triangles and connect the adjacent points by lines.

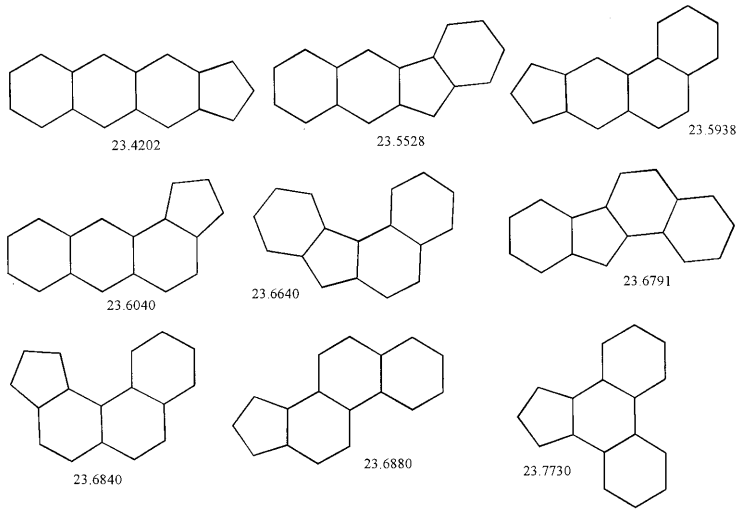

Fig. 11. The nine $C_{17}H_{11}$ fluorenoid isomers with their anionic π electronic energy listed below.

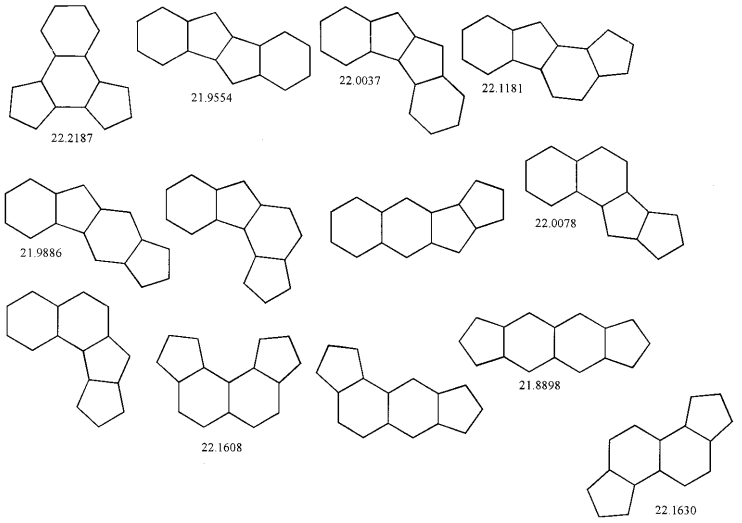

Fig. 13. The 13 indacenoid isomers of pyrene ($C_{16}H_{10}$).

$P \rightarrow L$:

$N_{Ic} \rightarrow r$ (empty), $N_c' = 3N_c - 3N_H + 6 - r_5$,
$N_H' = 2N_H - 6 + r_5$, $N_{pc} \rightarrow n_0'$,
$n_0 \rightarrow n_1'$, $n_1 \rightarrow n_2'$, $n_2 \rightarrow n_3'$,
$n_3 \rightarrow n_4'$, $n_4 \rightarrow n_5'$,

where N_{Ic}, N_{pc}, r (empty), and n_i are the number of internal degree-3, peripheral degree-3, rings without Clar sextets, and perimeter units ($i = 0$ for bay region, $i = 1$ for solo, $i = 2$ for duo, $i = 3$ for trio, $i = 4$ for quarto, and $i = 5$ for phenyl), respectively.

We now will show that the leapfrog transformation allows us to identify the most stable fluorenoid anions and indacenoid dianions within appropriate isomer sets. Using our prior algorithm [1], certain sets of fluorenoid / fluoranthenoid isomers can be generated from a corresponding known benzenoid isomer set as follows: One at a time, contract all distinct hexagonal rings in the molecular graphs belonging to a benzenoid isomer set of the formula C_nH_s with $N_{Ic} < 5$ to pentagonal rings and discard all duplicates to give all the fluorenoid / fluoranthenoid isomers of formula $C_{n-1}H_{s-1}$. In this way the five $C_{18}H_{12}$ benzenoid isomers give all nine of the $C_{17}H_{11}$ fluorenoid isomers presented in Figure 11. The corresponding HMO πp-electronic energy for the anions of these $C_{17}H_{11}$ fluorenoid isomers are listed below each structure in Figure 11. The anion of the last molecular graph, dibenzo[*e*,*g*]indenyl, has the largest HMO πp-electronic energy and HOMO-LUMO gap. The leapfrog of acenaphthylene, the only $C_{12}H_8$ fluoranthenoid, correctly identifies this last $C_{17}H_{11}$ fluorenoid as the most stable anion (Fig. 12).

Suppose you wish to find the structure of the most stable the fluorenoid monoanion $C_nH_s^-$ with a large number of isomers without examining or knowing each and every one of these isomers? As illustrated in the prior paragraph, this can be achieved by using the leapfrog operation on a smaller, possibly known, set of fluorenoids / fluoranthenoids ($C_{n'}H_{s'}$). To identify the formula of this smaller precursor set, one needs the equations

$$n' = \tfrac{1}{3}\, n + \tfrac{1}{2}\, s + 1 - \tfrac{1}{6}\, r_5,$$
$$s' = \tfrac{1}{2}\, s + 3 - \tfrac{1}{2}\, r_5.$$

If these equations do not give integral solutions, then none exist. For example, using these equations on the $C_{17}H_{11}$ formula for the fluorenoids in Fig. 12 gives $C_{12}H_8$ which corresponds to acenaphthylene in Figure 1.

We now illustrate the leapfrog transformation (Fig. 12) with the conversion of acenaphthylene ($C_{12}H_8$) to dibenzo[*e*,*g*]indenyl ($C_{17}H_{11}$). The omnicapping operation is done by placing a central point within each ring of acenaphthylene and connecting them to all adjacent ring vertices. The inner dualizing operation places a point within each triangle and joins them with lines (edges) to their neighboring points. The inner molecular graph shown in bold correspond to dibenzo[*e*,*g*]indenyl.

Taking the 9 molecular graphs in Fig. 11 and contracting all hexagonal rings one by one to pentagonal ones and discarding the duplicates give the 13 $C_{16}H_{10}$ indacenoid isomers of pyrene presented in Figure 13. Using the above equations and the leapfrog operation on benzo[*cd*]pentalene ($C_{11}H_7$) identifies the first molecular graph, benzo[*e*]-*as*-indacene, in Fig. 13 as being the most stable dianion.

Fluorenoid / Fluoranthenoid and Indacenoid Hydrocarbon Radicals

A number of important generalizations for fluorenoid / fluoranthenoid and indacenoid radicals systems can now be summarized. Like benzenoid hydrocarbons, odd-carbon fluorenoids / fluoranthenoids and indacenoids are always radical systems. The smallest fluoranthenoid diradical has the $C_{32}H_{14}$ molecular graph in Figure 3. Circumscribing this species once (Fig. 4) gives a monoradical ($C_{65}H_{19}$) and circumscribing it twice gives a nonradical species ($C_{108}H_{24}$). In comparison, successive circumscribing the smallest benzenoid diradical, triangulene ($C_{22}H_{12}$), at every stage gives successors that are diradicals [8]. The smallest indacenoid diradical has the $C_{30}H_{12}$ molecular graph in Fig. 6 and repetitively circumscribing it leads only to successors that are diradical species. Leapfrogging fluorenoids / fluoranthenoids always gives odd-carbon successors, and leapfrogging indacenoids always gives even-carbon successors. Contracting hexagonal rings to pentagonal ones tends to reduce the radical degree of polyradical species. For example, contracting one hexagonal ring to a pentagonal one in all monoradical benzenoids gives an even-carbon nonradical fluoranthenoid, and contracting two hexagonal rings to pentagonal ones in the triangular benzenoids as done in Fig. 5 reduces the radical degree by two. Thus, other things being equal, there is a tendency for fluorenoids / fluorantheoids, indacenoids, and polypent / polyhex systems

in general to have lower radical degree relative to benzenoids (polyhexes). This tendency by the presence of pentagonal rings in conjugated carbon systems to reduce the radical degree no doubt contributes to the driving force in the pyrolytic formation of fluoranthenoid and indacenoid hydrocarbons and fullerene carbons.

Conclusion

Using variation-from-average plots for ln *SC* versus the number of times circumscribed has facilitated our analysis of the topological matching properties between representative constant-isomer sets of fluoranthoid / fluorenoid and indacenoid hydrocarbons having the same isomer numbers. Leapfrogging polypent / polyhex systems with an odd number of pentagonal rings in addition to hexagonal ones give odd-carbon successors, and with even number of pentagonal rings give even-carbon successors.

Trimethylenemethane diradical and 2,5-dimethylenylpentalene diradical are excised internal structures of the smallest benzenoid diradical and indacenoid diradical, respectively. In analogy to the smallest D_{3h} polyradical benzenoids, a construction method for identifying the smallest fluoranthenoid / fluorenoid and indacenoid polyradicals has been presented. Two or more successive circumscribings of fluoranthenoid / fluorenoid diradicals or higher reduce them to alternating nonradical/monoradical series. In contrast, the radical degree of an indacenoid is preserved by at each successive circumscribing.

[1] (a) J. R. Dias, Chem. Phys. Lett. **185**, 10 (1991); (b) J. R. Dias, Chem. Phys. Lett. **187**, 334 (1991); (c) J. R. Dias, J. Chem. Inf. Comput. Sci. **32**, 2 (1992).

[2] (a) J. R. Dias, J. Chem. Inf. Comput. Sci. **32**, 203 (1992); (b) J. R. Dias, J. Chem. Inf. Comput. Sci. **35**, 148 (1995).

[3] (a) S. J. Cyvin, J. Molec. Struct. (THEOCHEM) **262**, 219 (1992); (b) S. J. Cyvin, B. N. Cyvin, and J. Brunvoll, J. Molec. Struct. (THEOCHEM) **281**, 229 (1993); (c) S. J. Cyvin, B. N. Cyvin, J .Brunvoll, Z. Fuji, G. Xiaofeng, and R. Tosic, J. Molec. Struct. (THEOCHEM) **285**, 179 (1993); (d) J. Brunvoll, B. N. Cyvin, S. J. Cyvin, G. Brinkmann, and J. Bornhoft, Z. Naturforsch. **51a**, 1073 (1996); (e) J. Brunvoll, B. N. Cyvin, and S. J. Cyvin, J. Chem. Inf. Comput. Sci. **36**, 91 (1996).

[4] (a) M. Gordon and W. H. T. Davison, J. Chem. Phys. **20**, 428 (1952); (b) M. Randić, J. Chem. Soc., Faraday Trans. 2, **72**, 232 (1976); (c) I. Gutman and S. J. Cyvin, Chem. Phys. Lett. **136**, 137 (1987); (d) S. J. Cyvin, and I. Gutman, Kekulé, Structures in Benzenoid Hydrocarbons, Springer-Verlag, Berlin 1988; (e) G. G. Hall, Chem. Phys. Lett. **145**, 168 (1988); (f) S. J. Cyvin, B. N. Cyvin, and J. Brunvoll, Chem. Phys. Lett. **156**, 595 (1989); (g) S. El-Basil and D. J. Klein, J. Math. Chem. **3**, 1 (1989); (h) C. Rongi, S. J. Cyvin, B. N. Cyvin, J. Brunvoll, and D. J. Klein, Top. Curr. Chem. **153**, 227 (1990); (i) S. J. Cyvin, B. N. Cyvin, J. Brunvoll, and I. Gutman, Monatsh. Chem. **122**, 771 (1991); (j) M. Randić, N. Trinajstić, L. L. Henderson, and R. P. Stout, J. Molec. Struct. (THEOCHEM) **285**, 121 (1993); (k) M. Randić, Y. Tsukano, and H. Hosoya, Nat. Sci. Rep. Ochanomizu Univ. **45**, 101 (1994); (l) T. Morikawa, Z. Naturforsch. **49a**, 511 (1994).

[5] (a) P. W. Fowler, J. E. Cremona, and J. I. Steer, Theor. Chim. Acta **73**, 1 (1988); (b) P. W. Fowler and D. B. Redmond, Theor. Chim. Acta **83**, 367 (1992); (c) D. E. Manolopoulos, D. R. Woodall, and P. W. Fowler, J. Chem. Soc. Faraday Trans. **88**, 2427 (1992); (d) P. W. Fowler, S. J. Austin, O. J. Dunning, and J. R. Dias, Chem. Phys. Lett. **224**, 123 (1994).

[6] (a) J. R. Dias, J. Chem. Inf. Comput. Sci. **31**, 89 (1991); (b) J. R. Dias, Chem. Phys. Lett. **176**, 559 (1991); (c) B. N. Cyvin, J. Brunvoll, and S. J. Cyvin, J. Chem. Inf. Comput. Sci. **32**, 72 (1992); (d) J. R. Dias, S. J. Cyvin, and J. Brunvoll, Polycycl. Arom. Comp. **2**, 195 (1991); (e) J. R. Dias, J. Chem. Inf. Comput. Sci. **39**, 144 (1999).

[7] (a) J. R. Dias, Theor. Chim. Acta **77**, 143 (1990); (b) J. R. Dias, J. Phys. Org. Chem. **3**, 765 (1990); (c) J. R. Dias, J. Molec. Struct. (THEOCHEM) **230**, 155 (1991); (d) J. R. Dias, J. Chem. Inf. Comput. Sci. **33**, 117 (1993).

[8] (a) J. R. Dias, Theor. Chim. Acta **81**, 125 (1991); (b) G. G. Cash, and J. R. Dias, J. Math. Chem., in press.

[9] D. J. Klein and X. Liu, J. Comp. Chem. **12**, 1260 (1991).

[10] V. R. Rosenfeld and I. Gutman, MATCH **24**, 191 (1989).

[11] J. M. Salvador, H. Hernandez, A. Beltran, R. Duran, and A. Mactutis, J. Chem. Inf. Comput. Sci. **38**, 1105 (1998).

[12] D. Babić, G. Brinkmann, and A. Dress, J. Chem. Inf. Comput Sci. **37**, 920 (1997).

[13] (a) D. E. Monolopoulos, Chem. Phys. Lett. **192**, 330 (1992); (b) X. Liu, T. G. Schmalz, and D. J. Klein, Chem. Phys. Lett. **192**, 331 (1992).

[14] S. J. Austin, P. W. Fowler, P. Hansen, D. E. Monolopoulos, and M. Zheng, Chem. Phys. Lett. **228**, 478 (1994).

[15] F. Fulop, A. Rockenbauer, F. Simon, S. Pekker, L. Korecz, S. Garaj, and A. Janossy, Chem. Phys. Lett. **334**, 233 (2001).